

Sources of L-Band RFI Determined from Kurtosis Using the SMAP Radiometer

D. M. Le Vine⁽¹⁾ and P. de Matthaëis^(1,2)

(1) Goddard Space Flight Center, Greenbelt, MD 20771 USA; e-mail: david.m.levine@nasa.gov

(2) University of Maryland, Baltimore County, Baltimore, MD 21250 USA; e-mail: paolo.dematthaei@nasa.gov

Abstract

Among the parameters of the signal measured by the SMAP radiometer to identify RFI is kurtosis which indicates the departure of the received signal from a gaussian distribution and therefore helpful in identifying RFI. But the kurtosis has the potential to provide additional information. This manuscript reports results of an investigation examining the connection between the level of kurtosis (K) and the characteristics of the source of the RFI. It is shown, for example, that the level of can be used to distinguish the short pulse, relatively wideband RFI associated with radar from the narrow bandwidth signals associated with faulty consumer electronics.

1 Introduction

Microwave remote sensing in the band 1400–1427 MHz (L-band) protected for passive measurements is important for global monitoring of soil moisture and sea surface salinity, parameters needed for understanding the global water cycle and climate change. Although emission in this band is prohibited, radio frequency interference (RFI) is observed over significant portions of the earth [1,2]. RFI means lost data and degraded science products and modern sensors employ algorithms to detect and remove RFI. But very little is known about the sources of the interference, even though information about the sources and the characteristics of the interference they generate has the potential to lead to improved detection.

The advanced tools for RFI detection system included in the SMAP radiometer [3] provide data to locate the source [4] and tools such as the spectrum and time history that can be used to relate the characteristics of the observed RFI with the characteristics of the source [5,6]. Among the parameters of the signal measured by the SMAP radiometer is kurtosis. Kurtosis measures the departure of the probability distribution (PDF) of a signal from a gaussian distribution. But kurtosis has the potential to provide additional information. Theory shows that the level (whether $K > 3$ or $K < 3$: $K = 3$ indicates a gaussian PDF) depends on the fraction of the radiometer integration cycle occupied by RFI, information which can be used to distinguish the short pulse relatively wideband RFI associated with radar from the narrow bandwidth signals associated with faulty consumer electronics. These conclusions have been verified using the SMAP signal to locate sources and comparing the kurtosis with the spectral

and temporal information provided by the SMAP radiometer.

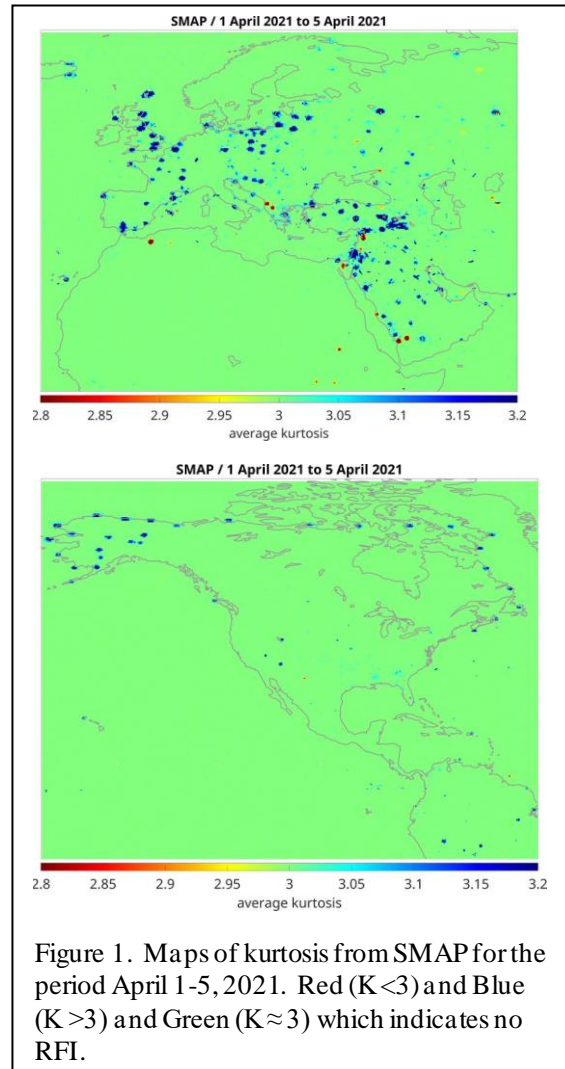


Figure 1. Maps of kurtosis from SMAP for the period April 1-5, 2021. Red ($K < 3$) and Blue ($K > 3$) and Green ($K \approx 3$) which indicates no RFI.

2 Background

The fundamental datum of the SMAP radiometer is a measurement at L-band (1400 MHz) averaged over an integration time of 0.3 ms and bandwidth of 24 MHz [3]. The radiometer is fully polarimetric with a coherent digital backend (i.e., phase and amplitude are preserved). In addition to the Stokes parameters, the kurtosis and spectrum of the signal are computed. Figure 1 is an example of the kurtosis reported by SMAP. RFI with $K > 3$

(blue) is dominant but there are also several cases of $K < 3$ (red). For example, red dots occur in the panel on the top along the west coast of the Red Sea and near Syria and near border of Morocco and Algeria. In the panel on the bottom, the blue dots ($K > 3$) running along the coast of Alaska and across Canada are associated with the radar of the North Warning System [7] which has been confirmed using the SMAP geolocation algorithm [4] but most sources are unknown.

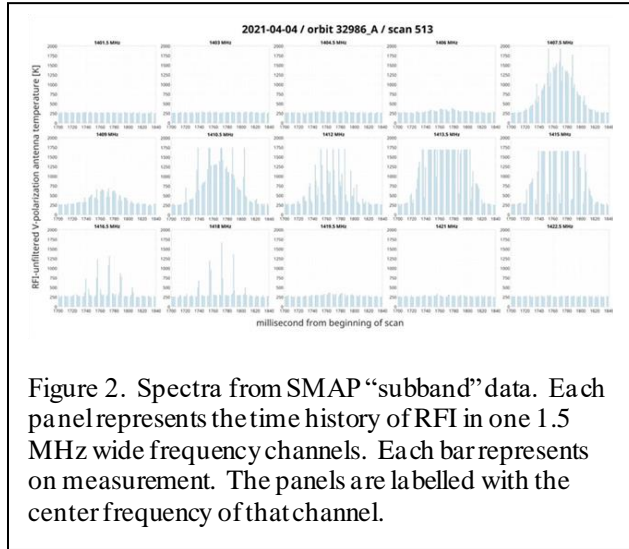


Figure 2. Spectra from SMAP “subband” data. Each panel represents the time history of RFI in one 1.5 MHz wide frequency channels. Each bar represents on measurement. The panels are labelled with the center frequency of that channel.

Figure 2 is an example of the spectrum provided by SMAP [3]. Each panel in Fig 2 represents the amplitude of the signal as a function of time in one of the frequency channels (each 1.5 MHz wide) starting at the top left with the channel with center frequency at 1401.5 GHz and ending at the bottom right with the channel at center frequency 1422.5 GHz. Each vertical bar represents one spectral measurement, and the spaces are the times set aside for radiometer internal calibration. In this example there is a strong source of RFI centered around 1700 ms which appears in several frequency bands. The RFI is strongest at 1413.5 MHz and 1415.0 MHz where the receiver is saturated.

Numerical simulations have been conducted to help understand the relationship between kurtosis and characteristics of RFI. It is assumed that the signal at the radiometer detector is a pulsed sinusoid plus a normally distributed random variable. The pulse represents the RFI and the random variable represents thermal emission from the surface which would be there in absence of the RFI. Specifically:

$$Y = A \text{rect}(t/T) \cos(2\pi f t + \phi) + R \quad (1)$$

where R is a normally distributed random variable, f is the frequency of the RFI, and $\text{rect}(t/T)$ is a rectangular pulse of unit amplitude and width $-T/1 < t < T/2$. This is the detected signal seen at the input to the radiometer backend digitizer. This signal is sampled at 96 mega samples/sec

for 0.3 ms (as done by SMAP [8]) and then the kurtosis is computed for each 0.3 ms measurement from the PDF of the samples. This can also be done theoretically. Determining the pdf of the discrete samples of a sinusoid in noise was solved by [9] and generalized to include a pulsed sinusoid by [10] (see Eqns 13-14 in [10]). In addition, [10] computed the kurtosis from these samples (Eqn 20 in [10]):

$$K = 3 (1+2S+S^2/2d)/(1+S)^2 \quad (2)$$

where d is the fraction of the radiometer integration time occupied by the sinusoid and S is the ratio of the amplitude A to the standard deviation. In (2), $K > 3$ when $d < 0.5$ and $K < 3$ when $d > 0.5$. The interpretation of the parameter “ d ” in (2) made by [10] is slightly different than made here, but the mathematics is applicable and (2) should be valid for the model investigated here. This has been confirmed numerically comparing K computed from the simulations (i.e., from the PDF of (1)) with K computed from (2). Saturation provides a real-world test of (2). Assuming $d = 1$ when the radiometer is in saturation, then (2) predicts $K = 1.5$ in the limit of very large S . The kurtosis reported by SMAP when the radiometer is in saturation is 1.3 - 1.7.

3 Discussion

In the relatively few cases where the sources of RFI is known, kurtosis $K > 3$ has been associated with radar. The prime example are the radar of the North Warning System, the blue dots in the right panel of Fig. 1 that extend along the coast of Alaska and across Canada. These include the AN/FPS 177 with pulse widths as short as 0.05ms and PRT longer than 1 ms which would suggest a high probability of $d < 0.5$ and therefore $K > 3$ which is what is seen in Fig. 1 (i.e., blue).

However, radar can also have $K < 3$ even when the signal does not saturate the radiometer receiver. An example is a very strong radar observed in China in 2020 [de Mattheis et al, 2021]. The spectrum of the RFI from this radar was very narrow band, appearing predominately in only one of the SMAP subbands (Fig. 6 in [11]) suggesting a relatively long pulse. The corresponding kurtosis was $K < 3$ (Fig. 7 in [11]) reaching 1.7 during saturation but remaining below 3 when the radiometer was not saturated.

To get more examples, a study was conducted of several sources selected from the map in the left panel in Fig 1 to determine if there was a correlation between the level of K and the spectrum observed by SMAP. Sources with $K > 3$ (blue) and $K < 3$ (red) were selected. Although the identity of each source was not known, the sources with wideband spectra (RFI appearing simultaneously in most channels) and suggestive of a short duration) were blue, and sources with narrow spectra (RFI appearing in only a few channels) and suggestive of longer pulses were red.

4 Conclusion

Based on a very limited supply of ground truth, a reasonable hypothesis is that strong RFI with $K < 3$ (and not saturated) is likely radar with pulses long compared to the SMAP radiometer integration time and when $K > 3$ the source is likely radar with pulses short compared to the integration time. RFI with $K \approx 3$ is likely a continuous, narrow band source of RFI. Several examples of faulty consumer electronics have recently been found by spectrum management officials given locations reported by SMAP including a surveillance camera in Wisconsin and an amplifier for a TV system in West Virginia. In each case the spectrum was narrow and kurtosis close to 3 [12].

References

- [1] D. M. Le Vine and P. de Matthaëis, "Aquarius active/passive RFI environment at L-band," *IEEE Geosci. Remote Sens. Lett.*, vol. 11, no. 10, pp. 1747–1751, Oct. 2014, doi 10.1109/LGRS.2022.3221888.
- [2] Y. Soldo, D. M. Le Vine, P. de Matthaëis, and P. Richaume, "L-band RFI detected by SMOS and Aquarius," *IEEE Trans. Geosci. Remote Sens.*, vol. 55, no. 7, pp. 4220–4235, Jul. 2017
- [3] Piepmeier, J.R., Johnson, J.T., Mohammed, P.N., Bradley, D., Ruf, C., Aksoy, M., Garcia, R., Hudson, D., Miles, L. and Wong, M., 2014. Radio-frequency interference mitigation for the soil moisture active passive microwave radiometer. *IEEE Transactions on Geoscience and Remote Sensing*, 52(1), pp.761-775, doi 10.1109/TGRS.2013.2281266.
- [4] Y. Soldo, D. M. Le Vine, A. Bringer, P. de Matthaëis, R. Oliva, J.T. Johnson, and J.R. Piepmeier, Location of Radio-Frequency Interference Sources Using the SMAP L-Band Radiometer, *IEEE Trans. Geosci. Remote Sens.*, vol. 56, no. 11, November, 2018.
- [5] Y. Soldo, R. Oliva, D. Le Vine, A. Bringer, P. de Matthaëis, Retrieval of RFI Characteristics Using L-Band Satellite Data, *International Geoscience and Remote Sensing Symposium*, pp 3766-3769. July, 2020 DOI: 10.1109/IGARSS39084.2020.9324281
- [6] Y. Soldo and D.M. Le Vine, Characteristics of the RFI environment at L-band as observed from SMAP, NASA/TM–20210000962, 2021, Avail from: National Technical Information Service, 5285 Port Royal Road, Springfield, VA 22161
- [7] NWS Northwest Warning System 2022 https://en.wikipedia.org/wiki/North_Warning_System
- [8] J. R. Piepmeier et al., "SMAP L-band microwave radiometer: Instrument design and first year on orbit," *IEEE Trans. Geosci. Remote Sens.*, vol. 55, no. 4, pp. 1954–1956, Jan. 2017, doi: 0.1109/TGRS.2016.2631978.
- [9] S. O. Rice, "Statistical properties of a sine wave plus random noise," *Bell Syst. Tech. J.*, vol. 27, no. 1, pp. 109–157, Jan. 1948.
- [10] R. D. De Roo, S. Misra, and C. S. Ruf, "Sensitivity of the kurtosis statistic as a detector of pulsed sinusoidal RFI," *IEEE Trans. Geosci. Remote Sens.*, vol. 45, no. 7, pp. 1938–1946, Jul. 2007.
- [11] P. de Matthaëis, D.M. Le Vine, Y. Soldo and A. Llorente, Study of a Strong L-Band RFI Source, *IEEE J. of Selected Topics in Applied Earth Observations and Remote Sensing*, JSTARS, Vol 14, 2021
- [12] D.M. Le Vine, P. de Matthaëis, P. Mohammed and J. Higgins, A Case Study in RFI at L-band Detected by SMAP, submitted to IGARSS 2023, Pasadena, CA July 2023.